A Low-Flicker Scheme for the Real-Time Measurement of Phase Noise

Enrico Rubiola and Vincent Giordano

Abstract—**This paper presents a new scheme for the measurement of phase noise in real time, based on carrier suppression and synchronous detection of the noise sidebands of the device being tested. In the instruments of the interferometric type, the carrier is suppressed by adding an equal and opposite signal that must be adjusted with a phase shifter and an attenuator. The proposed scheme makes use of a dual adjustment of the carrier suppression, coarse and fine. The former is by-step; the latter is continuous. Because of the higher stability of the by-step adjustment and the lower weight of the continuous adjustment in the suppression circuit, the instrument exhibits intrinsically low residual flicker and low microphonicity. A prototype shows a residual flicker as low as -160 dBrad^2/Hz at 1 Hz off the 100 MHz carrier. Applications include the noise characterization of components and the design of innovative ultrastable oscillators.**

I. Introduction

PHASE noise is generally described in terms of the power spectrum density $S_\varphi(f)$ of the random phase fluctuation $\varphi(t)$, as a function of the Fourier frequency f. This refers to a nearly perfect sinusoidal signal of carrier frequency ν_0 of the type $s(t) = V_0[1+\alpha(t)]\cos[2\pi\nu_0 t+\varphi(t)]$. In the field of frequency metrology, the amplitude fluctuation $\alpha(t)$ is often regarded as a minor problem.

Flicker noise $[S_\varphi(f) \propto f^{-1}]$ is probably the most difficult challenge in the design of ultrastable oscillators. In fact, according to the well-known Leeson model [1], the oscillator turns the phase flicker of its internal components into frequency flicker $[S_\varphi(f) \propto f^{-3}]$, which is a divergent process in the time domain. This paper proposes an innovative scheme of phase noise measurement instrument designed for the lowest residual flicker, intended for the measurement of components or for active noise removal, and it reports on a prototype that proves the benefits of the method.

A detailed analysis of the interferometric phase noise measurement method is reported in [2], together with microwave and HF-VHF design rules and experimental results. In addition, another recent paper [3] reports on the interferometric method, focusing on microwave applications. Hence, only a brief summary is given here.

With reference to Fig. 1, setting the attenuator ℓ and the phase shifter γ' equal to the device under test (DUT) attenuation and phase, the carrier is suppressed at the Δ port of the second 3 dB hybrid coupler. Therefore, only the DUT noise sidebands are present at the input of the amplifier. These sidebands are amplified, down converted to baseband, and measured by a fast Fourier transform (FFT) analyzer. Properly setting the phase lag γ'', the output voltage is $v(t) = k_\varphi\varphi(t)$, from which $S_\varphi(f) = S_v(f)/k_\varphi^2$. The phase-to-voltage gain is:

$$k_\varphi = \sqrt{\frac{R_0 g P_0}{\ell_h \ell_m}}, \tag{1}$$

where R_0 is the characteristic impedance the mixer output is terminated to, g is the power gain of the amplifier, P_0 is the carrier power at the DUT output, ℓ_h is the dissipative loss of the hybrid in the DUT-amplifier path, and ℓ_m is the single sideband (SSB) loss of the mixer.

The white noise floor of the instrument, as observed bypassing the DUT, is:

$$S_{\varphi 0} = \frac{2\ell_h F k_B T_0}{P_0}, \tag{2}$$

where F is the noise figure of the amplifier, $k_B = 1.38 \times 10^{-23}$ J/K is the Boltzmann constant, and T_0 is the room temperature; thus $k_B T_0 \simeq 4 \times 10^{-21}$ J, or -174 dBm/Hz.

The scheme of Fig. 1 differs from that of [2] in some minor details. The Σ port of the hybrid in the middle of the scheme is terminated to a resistance, and the mixer pump signal is derived from the main oscillator; thus, the DUT power can be changed by inserting an attenuator at the interferometer input without affecting the mixer pump level. Then, the adoption of 180° hybrids instead of the 90° ones shows technical advantages at frequencies below some 1 GHz, where lumped-parameter circuits are used, namely: higher isolation, lower dissipative loss, and wider bandwidth. Moreover, the hybrids can be successfully replaced with reactive impedance-matched power splitters. In order to avoid confusion, it should be noted that the power splitter, the hybrid coupler and the directional coupler (used in Section II) are three variations of the same basic 4-port device: the power splitter is a 3 dB hybrid coupler internally terminated at one port, and the directional coupler is a loosely coupled hybrid internally terminated at one port.

The scheme of Fig. 1 derives from [4] and [5]. Correlating and averaging the outputs of two interferometers that simultaneously measure a shared DUT results in improved sensitivity [6]. It has been demonstrated that, in this case, the residual noise derives from the difference between noise sources, and that thermal and nonthermal noise can be

Manuscript received July 10, 2001; accepted December 24, 2001.

E. Rubiola is with the ESSTIN and with the LPMI, Université Henri Poincaré, Nancy, France (e-mail: rubiola@esstin.uhp-nancy.fr).
V. Giordano is with the LPMO CNRS, Besançon, France.

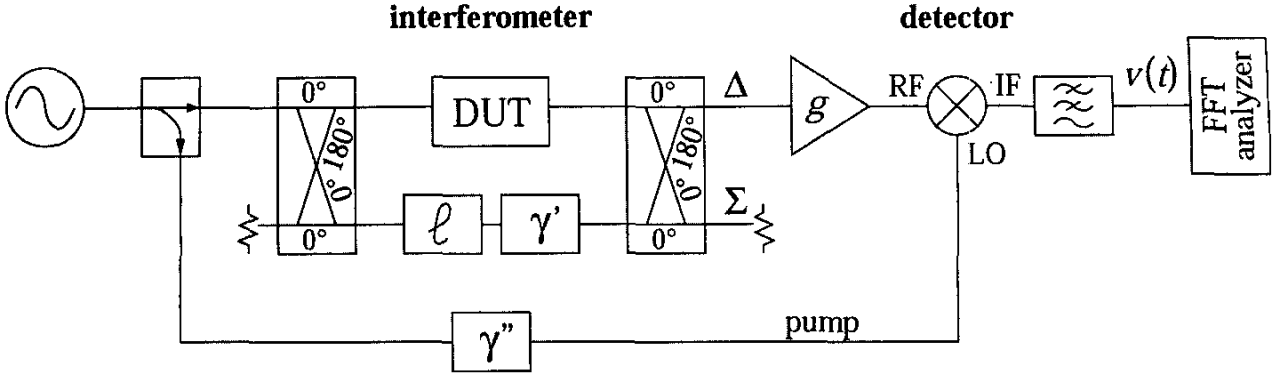

Fig. 1. Block diagram of the interferometric set-up for the measurement of phase noise.

strongly rejected if the noise sources are properly matched [7]. Yet averaged measures cannot be used for real-time applications.

II. The Dual Carrier Suppression Scheme

The close-to-the-carrier flicker of an amplifier comes from the near-dc flicker up-converted by nonlinearity. The nonlinear behavior of an amplifier stage can be represented in the time domain as the polynomial:

$$v_o(t) = a_0 + a_1 v_i(t) + a_2 v_i^2(t) + a_3 v_i^3(t) + \dots \quad (3)$$

truncated at the fourth order that describes the output voltage $v_o(t)$ as a function of the input signal $v_i(t)$. In our case, the input signal takes the form:

$$v_i(t) = V_0 \cos(2\pi\nu_0 t) + n(t), \quad (4)$$

where $V_0 \cos(2\pi\nu_0 t)$ is the carrier signal, and $n(t)$ is the equivalent input noise of the amplifier, that consists of near-dc flicker plus full-bandwidth white noise. Combining (3) and (4), the quadratic term turns out to be the major cause of the close-to-the-carrier flicker noise:

$$v_{o,2}(t) = 2a_2 V_0 \cos(2\pi\nu_0 t)\, n(t). \quad (5)$$

Commercial amplifiers are designed for telecommunication applications, in which the highest third order intercept point (i.e., the lowest a_3) is one of the most critical parameters; unfortunately, a_2 can be inferred in some cases only, and information related to the flicker component of $n(t)$ is never delivered.

Let us now consider a low-noise small-signal amplifier chain. Designing with commercial modules, the final scheme will (almost) necessarily be a chain of modules based on the same technology and having the same input and output impedance R_0 and the same supply voltage V_{CC}. Thus, the nonlinear coefficients are expected to be of the same order of magnitude. In this condition, flicker noise tends to arise from the output stage of the amplifier, where the residual carrier is stronger, rather than from the front-end. This noise mechanism has two consequences.

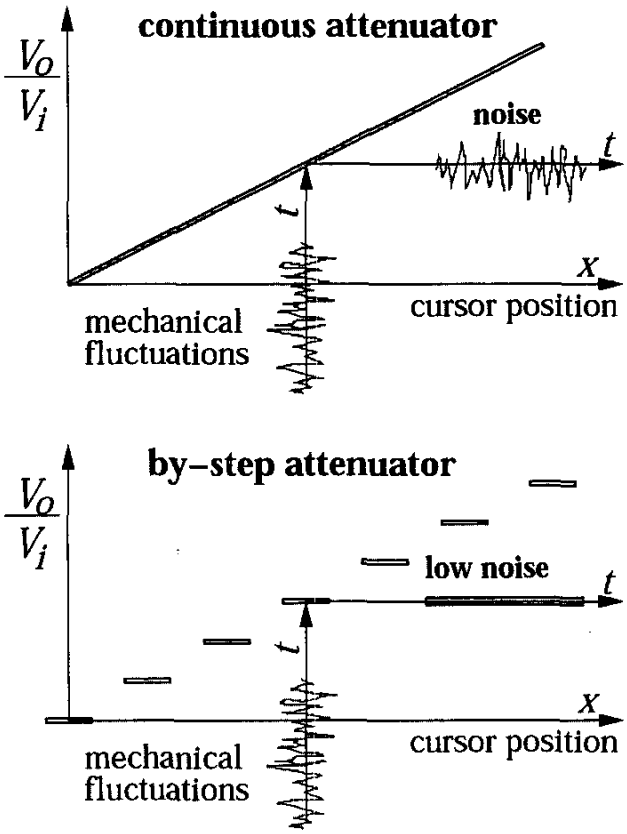

Fig. 2. Mechanical fluctuations of contacts turn into noise. A by-step attenuator compares favorably to a continuous one because contacts fluctuate on nearly equipotential surfaces.

The first one is that flicker noise cannot be predicted by the well-known Friis formula [8], that consists of evaluating the noise figure of a chain as the sum of the equivalent input noise of each amplifier divided by the gain of all the preceding stages. The second consequence is that the flicker of the amplifier can be minimized by keeping the residual carrier at the amplifier output stage as low as possible; thus the carrier suppression of the interferometer should be as accurate as possible. Therefore, the presence

of a fine adjustment path in addition to the main path ℓ-γ' is a desirable feature.

The flicker noise of the interferometer still remains, regardless of how low the residual carrier is. This is mainly due to the mechanical instability of the variable devices ℓ and γ', that induce random modulation. No advantage results from replacing these devices with electrically controlled attenuators and phase shifters, generally more noisy than the mechanically tunable ones. In some cases, the phase noise taken in by direct conversion of the fluctuation of the dc control voltage exceeds the device noise.

Experience and common sense suggest that a by-step attenuator more stable than a continuously variable one because nonperfect contacts fluctuate on a nearly equipotential surface, as heuristically shown in Fig. 2. Similarly, a by-step phase shifter is expected to be more stable than a continuous one. However, some difficulties are forecasted due to the insufficient resolution. In fact, letting $\Delta\varphi$ and $\Delta\alpha$ the phase and the amplitude imbalance, and neglecting losses, the carrier rejection at the interferometer output is $\Delta P/P_0 = (\Delta\alpha)^2+(\Delta\varphi)^2$. Searching through many technical catalogs, it seems that high quality 0.1 dB step attenuators are available from a few manufacturers, and a higher resolution is hard or impossible to find off the shelf. Thus, we take the carrier rejection of 45 dB as the limit that derives from the attenuator, assuming that the attenuation imbalance does not exceed half the 0.1 dB step. As for the phase shifter, a step of 11.6 mrad (i.e., 0.66°) is needed for a carrier rejection of 45 dB, still assuming that the imbalance never exceeds half the step. This corresponds to a step of 5.5 mm in length at the carrier frequency of 100 MHz, or to 4.4 mm in cable length if the signal propagates along cables at the velocity of 0.8 c. Although such a phase shifter is not available off the shelf, it can be implemented by switching—or by manually replacing—a set of semirigid cables. Consequently, the combined effect of the attenuator and phase shifter resolution yields a carrier rejection of some 42 dB in the worst case.

According to the design rules given in [2], a carrier rejection of 42–45 dB is generally insufficient to prevent the amplifier from flickering. The direct replacement of ℓ and γ' of Fig. 1 with actual by-step devices, therefore, is impossible. Yet, this difficulty is overcome with the scheme of Fig. 3, derived from [9]. The carrier is first attenuated by some 45 dB in the inner interferometer. This involves the by-step attenuator ℓ, the by-step phase shifter γ', and the two hybrids. The DUT noise sidebands, together with the residual carrier, are amplified by the first stage. Then, the carrier is almost completely suppressed in the outer interferometer by injecting a suitable signal at the output of the first amplifier; this involves the continuous attenuator ℓ_c, the phase shifter γ_c, and the directional coupler. Then, the DUT noise is further amplified and detected as in the previous scheme.

In summary:

- The first amplifier is prevented from flickering by ensuring its fully linear operation despite the carrier is suppressed only partially; this is done by selecting a device that exhibits a wide dynamic range and a relatively low gain.
- The output noise of the continuous attenuator and phase shifter, referred at the DUT output, is divided by $2\ell_h g'(k_c - 1)$, where k_c is the coupling parameter of the directional coupler, i.e., the inverse of the transmission coefficient. For the sake of simplicity, the dissipative loss of the coupler is not considered.
- The second amplifier is prevented from flickering by strongly reducing the residual carrier.

An alternate scheme is possible, in which the directional coupler through which the fine correction is injected is moved from the output to the input of the first amplifier; needless to say, the weight of the fine tune signal is preserved by changing k_c. Of course, this approach simplifies the choice of the first amplifier because it is no longer necessary to ensure the fully linear operation in the presence of the residual carrier that results from the coarse correction. However, the insertion loss of the directional coupler makes the equivalent noise figure of the amplifier increase by some 0.5–1 dB. Moreover, breaking the signal path at the amplifier input, where the signal level is the lowest, might result in increased sensitivity to mechanical vibrations and to electromagnetic pollution.

The dual-path carrier suppression scheme is more appealing than the simpler scheme in which ℓ and γ' are split into coarse and fine tune, cascaded along the signal path. In the latter case, the whole carrier power would cross the nonperfect contacts of the fine tune devices, and half of the resulting noise would be present at the amplifier input; thus, the benefit of dividing the contact noise by $2\ell_h g'(k_c - 1)$ would be lost.

The phase-to-voltage gain is:

$$k_\varphi = \sqrt{\frac{R_0 g' g'' P_0}{2\ell_h \ell'_h \ell_m \ell_{cp}}}, \tag{6}$$

independent of the choice of the fine correction point. ℓ'_h is the dissipative loss of the hybrid at the amplifier output; ℓ_{cp} is the insertion loss of the directional coupler, which accounts for both intrinsic attenuation and dissipative loss. The noise floor $S_{\varphi 0}$ is still given by (2), provided the loss ℓ_{cp} of the directional coupler be properly accounted in the noise figure F of the amplifier.

The presence of two detectors driven in quadrature makes the adjustment procedure simpler. Because of the dual detection, it is no longer necessary to calibrate the phase lag of critical cables by means of a network analyzer. A dual channel FFT analyzer is not actually necessary, unless the simultaneous measurement of $S_\alpha(f)$ and $S_\varphi(f)$ is needed for other reasons.

III. Prototype Implementation

The prototype we experimented on is designed to operate at the carrier frequency $\nu_0 = 100$ MHz. The inner interferometer is based on a 0.1 dB step attenuator and on

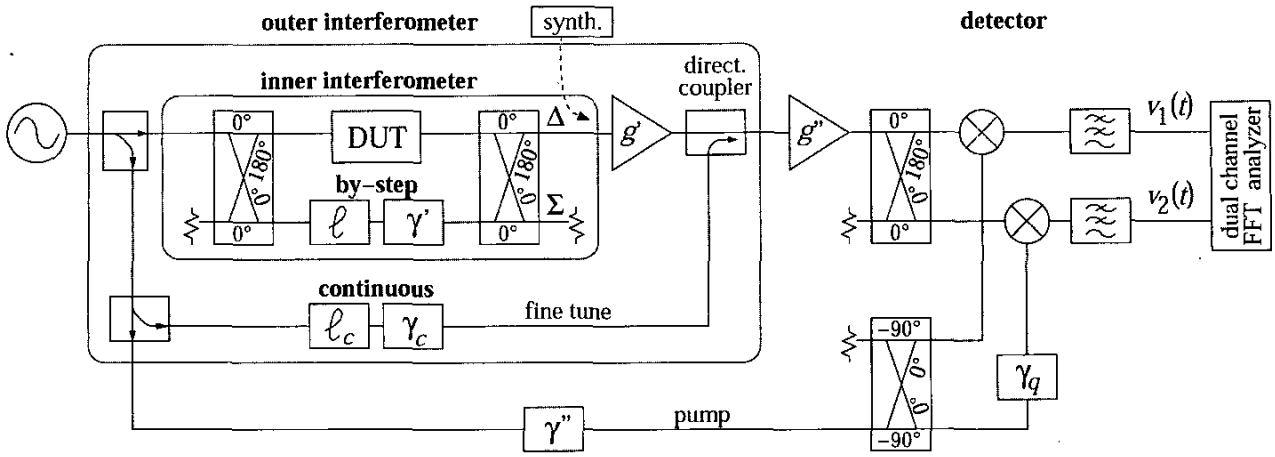

Fig. 3. Block diagram of the new interferometric set-up, based on dual carrier suppression.

a set of semirigid cables that plays the role of γ'. The hybrid loss is $\ell_h = 1$ dB, and the gain of the first amplifier is $g' = 11.8$ dB. The 100 MHz amplifier chain shows an overall gain of 40 dB and a noise figure $F = 2$ dB. The coupling of the fine correction is $k_c = 11.4$ dB. Consequently, the rejection of the continuous attenuator and phase shifter noise is $2\ell_h g'(k_c - 1) = 26.9$ dB. The dissipative loss of the hybrid at the amplifier output is $\ell'_h = 0.5$ dB, and the SSB loss of the mixer is $\ell_m = 6$ dB. The low pass filters that remove the $2\nu_0$ component show a cutoff frequency of 10 MHz and negligible loss up to 100 kHz, which is the maximum frequency of our FFT analyzer. A 40 dB low noise preamplifier (not shown), derived from the "super low noise amplifier" reported in [10], is inserted between each filter and the analyzer input. The 100 MHz source is a high stability oven controlled quartz oscillator followed by a power amplifier.

The adjustment and calibration procedure is straightforward. After removing the interferometer, the amplifier (g') is driven by a synthesizer that delivers a low-power sideband at a frequency ν_s close to ν_0; the fine tune signal is removed, and all unused ports are terminated. Hence, a beat note at the frequency $f_b = |\nu_0 - \nu_s|$ of a few kilohertz is present at the two outputs. In this condition, γ_q must be adjusted for the two outputs to be in quadrature by inspecting with the dual channel FFT analyzer. When the two outputs are in quadrature, the cross spectrum is imaginary, which can be best observed as a null of the real part. If a dual channel FFT is not available, the quadrature condition can be detected by means of a phase-meter, or by a lock-in amplifier that measures one output when it is synchronized to the other one. Then, the interferometer must be adjusted for the highest carrier rejection. This is accomplished first by inspecting the inner interferometer alone and acting on ℓ and γ', and then by restoring the final configuration and adjusting ℓ_c and γ_c for the lowest carrier power at the amplifier output. Subsequently, γ'' is set by observing the null of $v_1(t)$ when a reference phase modulator is inserted as the DUT. Thus, $v_1(t)$ is proportional to $\alpha(t)$ and $v_2(t)$ to $\varphi(t)$. Of course, the same phase modulation also is used for the direct measurement of k_φ. Then, the k_φ/k_α asymmetry—due to the imperfection of actual components—can be measured as the difference between the two output tone levels of the sideband measurement.

A carrier rejection of 80–90 dB can be obtained with our prototype, stable for about one hour. Operating with a DUT power $P_0 = 7.8$ dBm, the instrument shows a gain $k_\varphi = 64.6$ dBV/rad.

It is worthwhile to analyze how the phase and amplitude difference between the DUT and the phase modulator can affect the calibration. As long as the DUT and the phase modulator output are inserted at the same point and the phase γ'' is constant, the phase difference has no effect on the calibration; of course, the carrier suppression must be readjusted. A change in P_0 due to the attenuation difference affects k_φ; this can be corrected numerically with (6), or in hardware by inserting an attenuator. An alternate approach consists of the design of a low-loss modulator with an internal switch to select between the varactor and a fixed capacitor, i.e., calibration facility or lowest noise; that modulator can be let permanently as a part of the instrument.

IV. Experimental Results

Our main interest is the residual flicker noise of the instrument. Thus, we measured the noise spectrum $S_\varphi(f)$ in the absence of a DUT, that is bypassed.

The first experiment is intended to prove the validity of the basic assumption that the replacement of the continuous attenuator with a by-step one results in improved stability and lower flicker. Thus, the by-step attenuator is temporarily replaced with a continuous one. Fig. 4 compares the residual noise of the instrument. When the continuous attenuator is present (Fig. 4, left), the residual flicker is $S_\varphi(1\text{ Hz}) \approx -149$ dBrad^2/Hz, which is close to the result previously reported in [2], with a different instrument. That the $1/f$ amplitude noise is higher than its

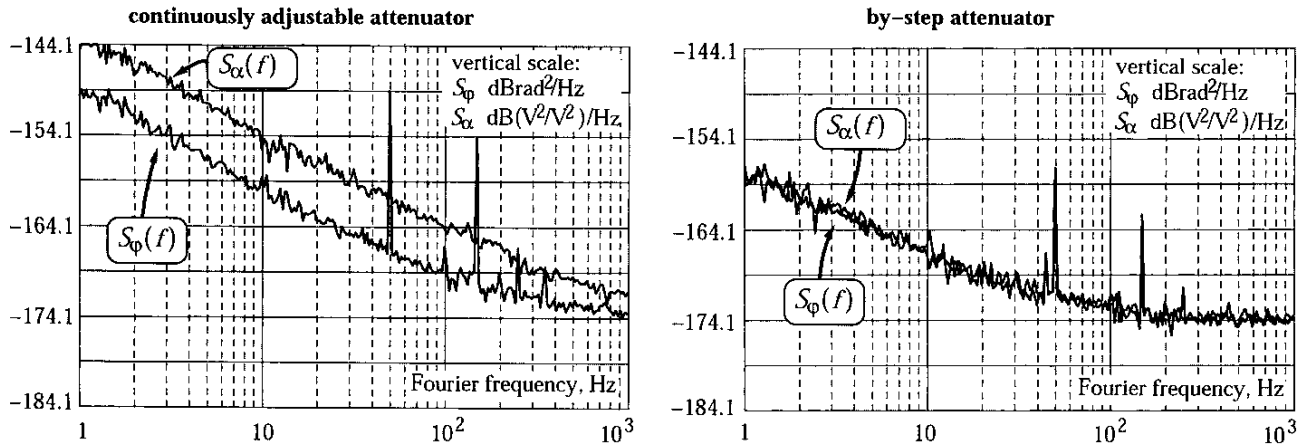

Fig. 4. Residual noise of the instrument, as observed changing the main attenuator ℓ from a continuously adjustable device to a by-step attenuator. Spectra are averaged over 13 acquisitions.

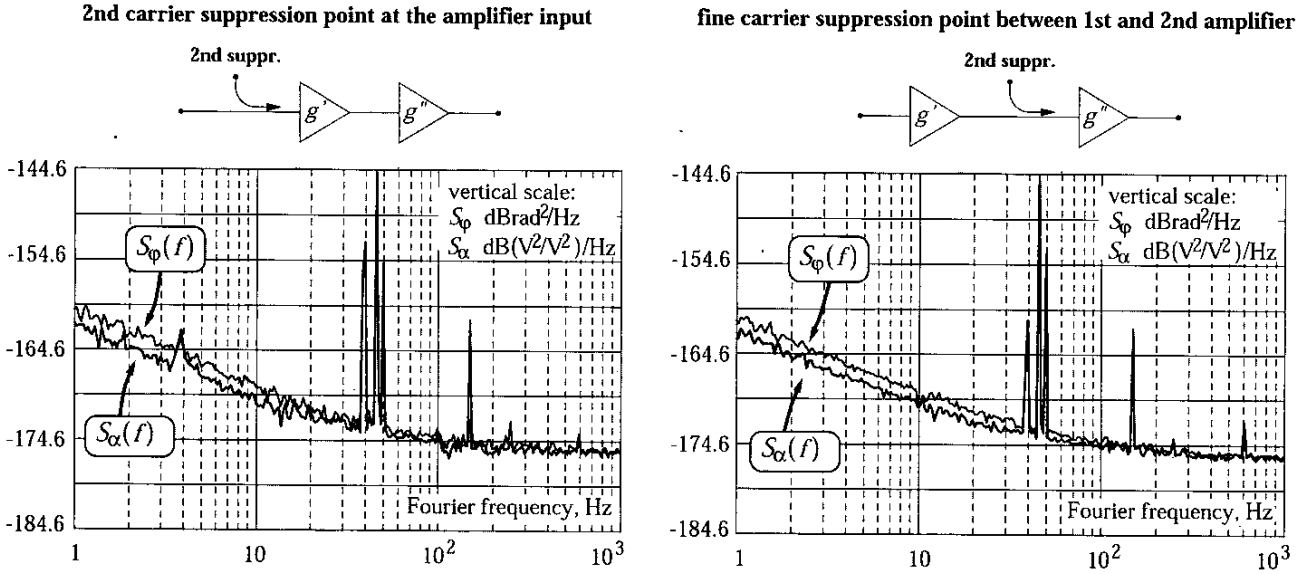

Fig. 5. Residual noise of the instrument, as observed changing the injection point of the fine carrier suppression signal. Averaging size: 25 acquisitions (left) and 52 acquisitions (right).

phase counterpart seems to confirm that the $1/f$ attenuator noise is of mechanical origin; as the phase change is a small stray effect of the cursor position—thus of the desired attenuation—on a macroscopic scale, on a microscopic scale mechanical fluctuations affect the insertion loss rather than the phase. After restoring the by-step attenuator (Fig. 4, right), the residual flicker $S_\varphi(1\text{ Hz})$ turns out to be some 9–10 dB lower. When the by-step attenuator is inserted, the amplitude noise $S_\alpha(1\text{ Hz})$ is almost equal to the phase noise.

In a second experiment, we compared the residual noise that results from the two choices of the fine carrier suppression point, at the input of the amplifier chain (Fig. 5, left) and between the first and the second stage (Fig. 5, right). The injection point at the output of the first stage yields a $S_\varphi(1\text{ Hz})$ some 2 dB lower, and a white noise floor some 0.5 dB lower, as compared with the injection between the two amplifiers. The difference in white noise is consistent with the increase in the amplifier noise figure that derives from the directional coupler. Injecting the compensation signal between the two stages results in a cleaner spectrum: stray signals (e.g., 50 Hz) are lower, and the mechanical resonance at $f = 4$ Hz vanishes. Nonetheless, the overall results are quite similar.

After improving some technical details—layout, ground path, etc.—we obtained the residual noise of Fig. 6. The white noise is -175.3 dBrad^2/Hz, which is close to the predicted value of -175.8 dBrad^2/Hz. The flicker noise is $S_\alpha(1\text{ Hz}) = -161.2$ dB(V^2/V^2)/Hz and $S_\varphi(1\text{ Hz}) = -160.3$ dBrad^2/Hz, in the same conditions.

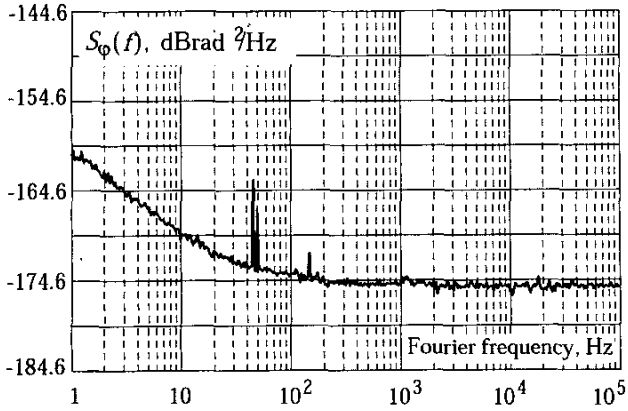

Fig. 6. Residual phase noise of the instrument, after optimization. Spectrum is averaged over 60 acquisitions.

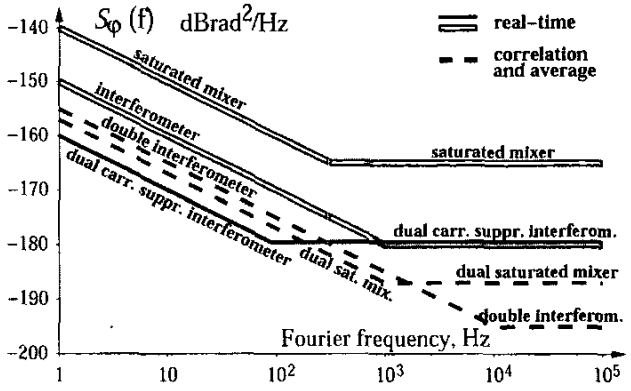

Fig. 7. Comparison between the residual noise of known instruments and methods.

V. Final Remarks

The residual flicker of this instrument improves some 10 dB upon the previous interferometer [2], and some 5 dB upon the double interferometer [6], [7]. This is a remarkable performance because the double interferometer makes use of two independent amplifiers and two independent interferometers to remove the instrument noise by correlation, and makes the noise spectrum available only after a long averaging time.

A residual flicker of some -160 dBrad^2/Hz at 1 Hz off the carrier represents the highest sensitivity ever reported for an instrument that measures phase noise in real time in the radiofrequency and microwave bands.

We wish to stress that no attempt has been made to exploit data processing techniques to hide the spectral lines due to mechanical vibrations and to the interferences from the mains, and that a moderate averaging has no effect on them. All the experiments were done in a laboratory room not shielded, and without environmental parameter control. Although lead-acid batteries were present in parallel to the power supply for backup purpose, we did not disconnect the ac power supply during the final measurements. The low level of the stray signals that appears in Fig. 6 is due to:

- a good mechanical assembly,
- the intrinsic immunity to the low frequency magnetic fields that derives from the amplification of the noise sidebands before detecting,
- the increased mechanical stability that results from having removed the continuously variable attenuator and phase shifter from the critical path.

For comparison, Fig. 7 reports the residual noise of some instruments for the measurement of phase noise. The saturated mixer refers to general experience, in a favorable case; the interferometer refers to [2], at $\nu_0 = 100$ MHz; the dual saturated mixer refers to [11] at $\nu_0 = 5$ MHz; the double interferometer refers to [6], [7], at $\nu_0 = 100$ MHz.

The described instrument measures the instant value of $\varphi(t)$ in real time, which can be exploited for the dynamic correction of the noise of oscillators and amplifiers, as suggested in [3] for microwave applications.

Similar results are expected in a wide frequency range, from 1 MHz or less to a few hundreds of megahertz, where the same technology is available and a reasonable resolution of γ' is feasible.

Considering a microwave implementation, an obvious difficulty arises from the resolution of the phase shifter γ'. A fixed phase shifter, machine- or laser-trimmed, seems the most appealing solution. Of course, this fixes γ', which limits the application to single-DUT instruments, as it occurs in the the dynamical noise correction circuits.

References

[1] D. B. Leeson, "A simple model of feed back oscillator noise spectrum," in *Proc. IEEE*, vol. 54, pp. 329–330, 1966.

[2] E. Rubiola, V. Giordano, and J. Groslambert, "Very high frequency and microwave interferometric PM and AM noise measurements," *Rev Sci. Instrum.*, vol. 70, pp. 220–225, Jan. 1999.

[3] E. N. Ivanov, M. E. Tobar, and R. A. Woode, "Microwave interferometry: Application to precision measurements and noise reduction techniques," *IEEE Trans. Ultrason., Ferroelect., Freq. Contr.*, vol. 45, pp. 1526–1535, Nov. 1998.

[4] K. H. Sann, "The measurement of near-carrier noise in microwave amplifiers," *IEEE Trans. Microwave Theory Tech.*, vol. 9, pp. 761–766, Sep. 1968.

[5] F. Labaar, "New discriminator boosts phase noise testing," *Microwaves*, vol. 21, pp. 65–69, Mar. 1982.

[6] E. Rubiola, V. Giordano, and J. Groslambert, "Improved interferometric method to measure near-carrier AM and PM noise," *IEEE Trans. Instrum. Meas.*, vol. 48, pp. 642–646, Apr. 1999.

[7] E. Rubiola and V. Giordano, "Correlation-based phase noise measurements," *Rev. Sci. Instrum.*, vol. 71, pp. 3085–3091, Aug. 2000.

[8] H. T. Friis, "Noise figure of radio receivers," in *Proc. IRE*, vol. 32, pp. 419–422, July 1944.

[9] E. Rubiola and V. Giordano, "Dual carrier suppression interferometer for the measurement of phase noise," *Electron. Lett.*, vol. 36, pp. 2073–2075, Dec. 7, 2000.

[10] Analog Devices (formerly Precision Monolithics Inc.), specification of the MAT-03 low noise matched dual PNP transistor. Also available as mat03.pdf from the web site http://www.analog.com/.

[11] W. F. Walls, "Cross-correlation phase noise measurements," in *Proc. 46th Freq. Contr. Symp.*, 1992, pp. 257–261.

Enrico Rubiola was born in Torino, Italy, in 1957. He graduated in electronic engineering in 1983 at the Politecnico, the technical university of Torino, and received the Ph.D. in Metrology in 1988 from the Italian Ministry of Scientific Research in Rome. After having been a reasearcher at Politecnico and a professor at the Universty of Parma in Italy, he is a professor within the Université Henri Poincaré (UHP) in Nancy, France. Prof. Rubiola is a researcher at the LPMIA, the Laboratory of Physics of Ionized Media and Applications at the UHP, and he teaches electronics at the ESSTIN (Ecole Supérieure de Sciences et Technologies de l'Ingénieur de Nancy), the state engineering school within the UHP, where he is head of the Department of Electronics.

Enrico Rubiola has worked on various topics of electronics and metrology, namely, navigation systems, time and frequency comparisons, atomic frequency standards, and gravity. His main fields of interest are precision electronics and phase noise metrology, which include frequency synthesis, high spectral purity oscillators, and noise.

Vincent Giordano was born in Besançon, France, on February 20, 1962. He received the Engineer degree in 1984 from the Ecole Supérieure de Mécanique et des Microtechniques, Besançon, France, and his Ph.D. in Physical Sciences in 1987 from the Paris XI University, Orsay, France.

During 1984–1993, he was a researcher of the permanent staff of the Laboratoire de l'Horloge Atomique, Orsay, France, where he worked on a laser diode optically pumped cesium beam frequency standard. In 1993, he joined the Laboratoire de Physique et de Métrologie des Oscillateurs (LPMO), Besançon, France, where he is the head of the Microwave Metrology team. Presently, his main area of interest is the study of high spectral purity microwave oscillators and the high sensibility phase noise measurement systems.